TELKOMNIKA Telecommunication, Computing, Electronics and Control
Vol. 19, No. 2, April 2021, pp. 690~704
ISSN: 1693-6930, accredited First Grade by Kemenristekdikti, Decree No: 21/E/KPT/2018
DOI: 10.12928/TELKOMNIKA.v19i2.18155

Roof materials identification based on pleiades spectral responses using supervised classification

Ayom Widipaminto[1], Yohanes Fridolin Hestrio[2], Yuvita Dian Safitri[3], Donna Monica[4], Dedi Irawadi[5], Rokhmatuloh[6], Djoko Triyono[7], Erna Sri Adiningsih[8]
[1,2,3,4,5,8]Remote Sensing Technology and Data Center, National Institute of Aeronautics and Space, Indonesia
[1,6,7]Department of Physics, Faculty of Mathematics and Sciences, University of Indonesia, Indonesia

Article Info

Article history:

Received Aug 7, 2020
Revised Nov 12, 2020
Accepted Nov 25, 2020

Keywords:

Classification
Machine learning
Reflectance response
Roof materials
Satellite imagery

ABSTRACT

The current urban environment is very dynamic and always changes both physically and socio-economically very quickly. Monitoring urban areas is one of the most relevant issues related to evaluating human impacts on environmental change. Nowadays remote sensing technology is increasingly being used in a variety of applications including mapping and modeling of urban areas. The purpose of this paper is to classify the Pleiades data for the identification of roof materials. This classification is based on data from satellite image spectroscopy results with very high resolution. Spectroscopy is a technique for obtaining spectrum or wavelengths at each position from various spatial data so that images can be recognized based on their respective spectral wavelengths. The outcome of this study is that high-resolution remote sensing data can be used to identify roof material and can map further in the context of monitoring urban areas. The overall value of accuracy and Kappa Coefficient on the method that we use is equal to 92.92% and 0.9069.

Corresponding Author:

Ayom Widipaminto
Remote Sensing Technology and Data Center
National Institute of Aeronautics and Space
Jakarta, Indonesia
Email: ayom.widipaminto@lapan.go.id

1. INTRODUCTION

Urban areas are now a type of land cover that is changing very rapidly, even though these areas only meet a low percentage of the entire land surface globally [1, 2]. The urban environment is also dynamic and experiences rapid physical and socio-economic changes [3]. Urban area planning requires information from various phenomena and spatial characteristics such as roof materials, urban structures, and building resilience [4]. Built-up land monitoring in more detail about land use will describe the development of the city area [5]. Built-up land monitoring to detail the type of roof material can also describe in more detail the economic level of the community. Knowledge of roof materials types also makes it possible to establish quantification monitoring of pollutant emissions from hazardous materials [6]. Roof materials type information also needed for the development of photovoltaic potential, used to build a micro weather model simulator, and is needed for the military to determine the type of air attack, urban planning, and disaster assessment [7-9]

Monitoring urban areas is one of the most relevant issues related to evaluating the impact humans have on the environment. In current remote sensing, imagery has many benefits, one of which can produce the latest geographic data for needs such as land use mapping, emergency response management, roof

locations with high and low emissivity, a better understanding of greening initiatives, and sustainable city development [10]. Remote sensing technology is increasingly being used in a variety of applications including mapping and modeling of urban areas. Driven by technological advancements and community needs, remote sensing in urban areas is increasingly becoming a new arena of geospatial technology and has the application of benefits in all socio-economic sectors [11]. The spatial resolution used for identification greatly influences the output produced. So far, remote sensing data that are widely used in land and urban observations still use medium resolution image data such as Sentinel-2 [12] and Landsat-8 [13], where Sentinel-2 and Landsat-8 have a resolution of around 10m and 30m. This results in inaccurate identification because urban areas are so varied and dynamic that higher image resolution is needed. This is reinforced by the existence of new facts or paradigms that very high-resolution data needs to be adopted to produce satisfactory image analysis [14].

The identification method used in this paper is spectroscopy - the study of electromagnetic radiation. Imaging spectroscopy has many names in the remote sensing community, including imaging spectrometry, hyperspectral, and ultra-spectral imaging. Spectroscopy is a technique for obtaining spectrum or wavelengths at each position from various spatial data so that images can be recognized based on their respective spectral wavelengths. The picture can be a rock in a laboratory, a field study on an airplane, or an entire planet from a spacecraft or an Earth-based telescope. By analyzing spectral features, and thus specific chemical bonds in a material, one can map where those bonds occur, and thus map the material [15]. The purpose of this paper is to classify the types of materials based on their spectral responses, as a basis for the identification of roof materials. Our contribution is the use of Pleiades data, very high-resolution satellite data with a multispectral resolution that has not been used by current conditions.

2. RESEARCH MATERIALS AND METHOD

2.1. Literature study

Previous research on the collection of spectral libraries for the detection of urban material has been discussed in several papers such as, in [3] they were combining spectral and spatial attributes, classification is done in two ways namely per-pixel (guided classification) and object-based (oriented object), in [2] which compares the ability of different sensors to detect material cover in urban areas by evaluating and also adding hyperspectral sensor values to map urban areas. A new approach has also been taken to determine and evaluate strong spectral features against spectral overlaps between material classes and class variability. The robustness of interactively determined spectral features was evaluated by separation analysis. This method is done based on the confusion matrix for each material that is calculated from each classification result [16]. DAIS (digital aerial imaging spectrometers) Hyperspectral data and ROSIS (reflective optical system imaging spectrometers) have been used for data extraction with several approaches for urban areas (spatial information) and non-urban areas (spectral information) [17]. Research in [18] has developed automated methods for hyperspectral image analysis that can exploit spectral and spatial information content thoroughly from data to distinguish types of urban surface coverings using mathematical models that can reduce the value so that it will be possible endmember combinations for each pixel by introducing pure spectral seedlings and registering possible endmember combinations for adjacent pixels in the unmixing procedure.

Research conducted in [6] creates a super spectral sensor design for the classification of urban material, band selection is carried out to identify the most optimal subset of bands to classify urban maps in the context of super spectra sensor design by collecting spectral categories for urban material from seven spectral libraries (using hyperspectral data and ground truth). The invariant formula for spectral images of natural objects retains spectral information and does not differ from highlights, shadows, surface geometry, and lighting intensity and also proves that conventional spectral invariant techniques can be applied to metals other than dielectric objects [19]. The combined performance of data mining (DM) and object-based image analysis (OBIA) develops procedures that contribute to automatic knowledge discovery and mapping of urban surface material from images of large hyperspectral space features with an accuracy of 88% [20]. Research in [21] has built a spectral library of urban materials and uses them to analyze urban environments with a comprehensive collection of spectral reflectance of various urban materials, resulting in an accuracy of 73% using maximum likelihood. Then, from studies conducted by [22], spectrometers and VNIR (visible and almost infrared) cameras produce different spectral reflectance values even though the targets are the same. Figure 1 shows the spectral profile of the roof and surface material, and Figure 2 shows the surface reflection of a selective urban surface material recorded by the Hyperspectral HyMap sensor as a reference for this study.

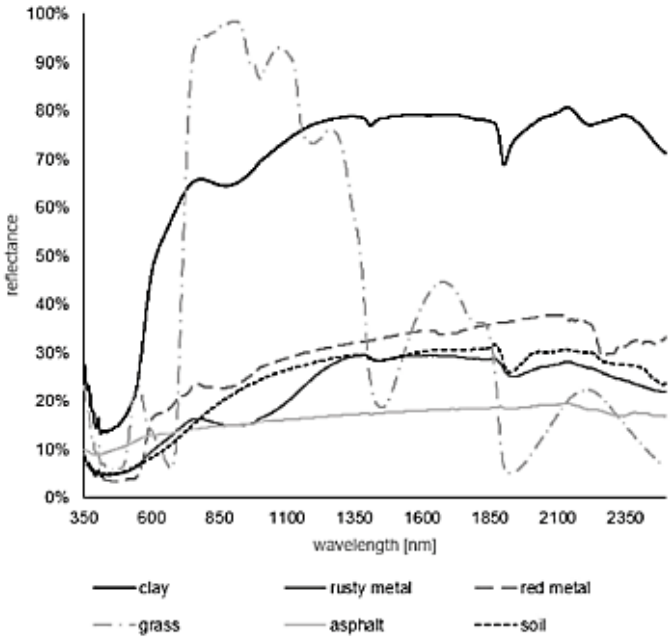

Figure 1. Spectral profiles of roof and surface materials [23]

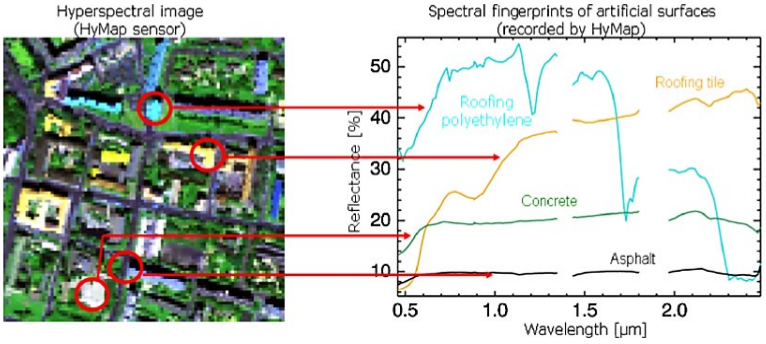

Figure 2. At surface reflectance of selective urban surface materials recorded by the hyperspectral HyMap sensor [24]

2.2. Location and data

The research area is located at the Remote Sensing Technology and Data Center, National Institute of Aeronautics and Space, East Jakarta. Roof sampling is carried out in the Remote Sensing Technology and Data Center building which has a variety of materials including aluminum roof, asbestos, ceramic tile, concrete, and sand metal tile. Figure 3 shows the image we used in this study. The noise could affect data quality [25, 26, 27, 28, 29], especially image quality in this research. Instead of discussing low-quality images, we choose high-resolution images. Therefore, the data used for this study is cloud-free image data from the Pleiades satellite obtained on 1 May 2018. Representative spatial and temporal resolution sensors for the satellite are described in Table 1.

Table 1. Representative spatial and temporal resolution sensors [30]

Sensor	Band Type	Spatial Resolution	Global Revisit Cycle	Operational Period	Access
Pleiades	Panchromatic Multispectral	50 cm 2 m	Daily	2011-present (Pleiades-1A) 2012-present (Pleiades-1B)	Commercial

Figure 3. Study area

2.3. Method

The method that we propose was carried out as follows. First, we obtained the data used in this study, Pleiades satellite imagery. We filter data to 0% cloud cover with an angle of view that less than 20°. The data then processed into a pan-sharpened multispectral (PMS) using the Ehlers method [31]. The next step of our method is to get training data by selecting pixels from the data. Training data is selected by cluster sampling method and sampling with a harmonious system where each sample has pixel spaces. Cluster sampling is used to categorize material types while systematic sampling is used to take the representation of adjacent pixels. We selected training data for each type of roof material, namely aluminum roof, asbestos, ceramic tile, concrete, and sand metal tile. Clustering was done using a multi-core cluster, the use of the cluster is automatic in these functions. The library that we used is particularly useful to speed up computations in functions like predict, interpolate, and perhaps calc [32].

The next stage is the selection of features by extracting the reflectance value of each pixel of the image. At this stage, the value of each pixel (range 16 pixels 0-65535) of the data obtained is read to calculate the emission and reflection values using formula (3) and (4). After data collection and feature selection, next is the classification using the support vector machine (SVM) classification method - a machine learning (ML)-based classifier which is established based on the statistical learning theory [33]. In this study, we used SVM since SVM is rarely used for remote sensing image classification. For the SVM ML models, we adapt the models from random forest ML from [34], we take the species distribution modeling to apply it using SVM for ML. We use C-classification (multi-class classification) for the SVM-type, the SVM kernel is radial basis function [35, 36, 37]. The C-classification and SVM-kernel (radial basis function) formulas are expressed in the (1) and (2).

C-classification:

$$\begin{aligned} &\min_{\alpha} \quad \frac{1}{2}\alpha^{\top}\mathbf{Q}\alpha - e^{\top}\alpha \\ &s.t. \quad 0 \le \alpha_i \le C, \mathrm{I} = 1, \ldots, l, \\ &y^{\top}\alpha = 0 , \end{aligned} \tag{1}$$

where $\boldsymbol{e}$ is the unit vector, C is the upper bound, $\boldsymbol{Q}$ is an l by l positive semidefinite matrix, $Q_{ij} \equiv y_i y_j K(x_i, x_j)$, and $K(x_i, x_j) \equiv \phi(x_i)^{\top}\phi(x_j)$ is the kernel [38]. SVM-Kernel, radial basis function [39]:

$$K(x_1, x_2) = \exp(-\gamma \|x_1 - x_2\|^2) \tag{2}$$

We classify our data into five classes of types of roof materials, namely aluminum roof, asbestos, ceramic tile, concrete, and sand metal tile. Finally, the evaluation was done by visually comparing the results of the classification with satellite images. The whole study method is illustrated in the diagram in Figure 4.

Figure 4. Research diagram

2.3.1. PMS Process

PMS was done with the following steps:

- Input data that contain panchromatic data level sensor primary, multispectral data level sensor primary, and digital elevation model (DEM) data of the area of interest (AOI) region with the same resolution as panchromatic resolution or higher.
- The orthorectification process uses DEM data.
- Pansharpening process between panchromatic and multispectral.

The pansharpening method used was the University of New Brunswick's which was developed by Dr. Yun Zhang. This method can produce images with good consistent quality for all sensors. This has been evaluated and analyzed with nine comparison algorithms [40].

- Convert Digital Count to Top of Atmosphere (TOA) Radiance.

For a respective band (b), the conversion of the Digital Count of a pixel DC(p) to TOA radiance $L_b(p)$ (in W·sr−1·m−2·μm−1) is done by the absolute radiometric calibration coefficients GAIN and BIAS [41]:

$$L_b(p) = \frac{DC(p)}{GAIN(b)} + BIAS(b) \quad (3)$$

- TOA Radiance to TOA Reflectance process

The Top Of Atmosphere (TOA) spectral reflectance is the ratio of the TOA radiance normalized by the incoming solar irradiance [41]. The output data is a pan-sharpened multispectral data level ortho standard.

$$\rho_b(p) = \frac{\pi \,.\, Lb(p)}{Eo(b) \,.\, \cos(\theta s)} \quad (4)$$

3. RESULTS AND ANALYSIS

First, we obtained 734 training data from Pleiades images, as shown in Figure 5. The number of detailed training data per material is shown in Table 2. The training data that we use was the area that was directly exposed to the sun caught in the satellite data. For the features used in the classification, spectral data were obtained for 5 (five) types of roof material from high-resolution satellite imagery, i.e. aluminum roof, asbestos, ceramic tile, concrete, and sand metal tile. The measurement of the roof shows a unique spectral sign which can be seen in Table 3. For better understanding, we analyze the spectral response line graphs as shown in Figure 6 (a). Reflectance is used in the analysis since reflectance is a property of the target material itself. It measures how much energy (as a percent) a surface reflects at a specific wavelength [42]. Many surfaces reflect a different amount of energy in different portions of the spectrum. These differences in reflectance make it possible to identify different earth surface features or materials by analyzing their spectral reflectance signatures [43]. Spectral reflectance values are also easier to read and understand as a classification because they have a range value of 0-1.

From the scatter plot in Figure 6 (b), it can be seen that the spectral values we calculated are quite narrow for each band except for the spectral response of NIR bands that have a large enough standard deviation. It shows that the spectral response in the red band is generally lower than the other bands and increases significantly in the NIR band. The scatter plot result between the bands also shows that the overall band shows a significant distribution to the NIR band, especially the red band that has the most dominant result when facing the NIR band. This behavior seems to be unique in every material and therefore can be used as a feature to distinguish between one material and another.

After that, we proceed with the classification using SVM. Using the training data, we obtained a classification model with an accuracy of 94.01% and a Kappa coefficient of 0.9165. Then this SVM Model is used to classify Pleiades data that is used comprehensively, the results of which are shown in Figure 6 (c). Pleiades data used were successfully classified into five classes, where classes 1, 2, 3, 4, and 5 each represented aluminum roof, asbestos, ceramic tile, concrete, and sand metal tile. We perform SVM confusion matrix calculations to show the results of machine learning in identifying roof material (Table 4). It can be seen in the table that SVM detects differences in training data with ML results on asbestos and sand metal tile materials. We also provide SVM statistics per class and SVM receiver operating characteristic (ROC) class as shown in Table 5 and Figure 7. In general, the classification correctly identifies the material around the study area described in Figure 8.

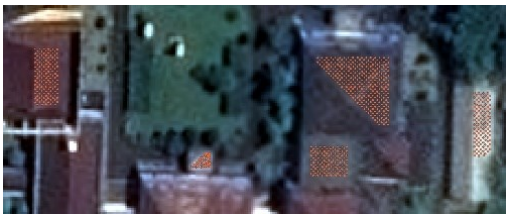

Figure 5. Training data collected from the image

Table 2. Details of training data used

Materials	Pleiades training data
Aluminum Roof	114
Asbestos	119
Ceramic Tile	143
Concrete	42
Sand Metal Tile	316

Table 3. Unique spectral signs of each material

Materials	Band Reflectance Value			
	Blue	Green	Red	NIR
Aluminum Roof	0.322	0.299	0.276	0.334
Asbestos	0.234	0.204	0.183	0.237
Ceramic Tile	0.215	0.184	0.192	0.260
Concrete	0.317	0.275	0.253	0.390
Sand Metal Tile	0.220	0.187	0.167	0.222

Table 4. SVM confusion matrix

Prediction	Actual				
	Aluminum	Asbestos	Ceramic tile	Concrete	Sand metal tile
Aluminum	114	0	0	0	0
Asbestos	0	90	0	0	15
Ceramic Tile	0	0	143	0	0
Concrete	0	0	0	42	0
Sand metal tile	0	29	0	0	301

Table 5. SVM statistics by class

Class:	Aluminum	Asbestos	Ceramic tile	Concrete	Sand metal tile
Sensitivity	1.0000	0.7563	1.0000	1.00000	0.9525
Specificity	1.0000	0.9756	1.0000	1.00000	0.9306
Pos Pred Value	1.0000	0.8571	1.0000	1.00000	0.9121
Neg Pred Value	1.0000	0.9539	1.0000	1.00000	0.9629
Prevalence	0.1553	0.1621	0.1948	0.05722	0.4305
Detection Rate	0.1553	0.1226	0.1948	0.05722	0.4101
Detection Prevalence	0.1553	0.1431	0.1948	0.05722	0.4496
Balanced Accuracy	1.0000	0.8660	1.0000	1.00000	0.9416

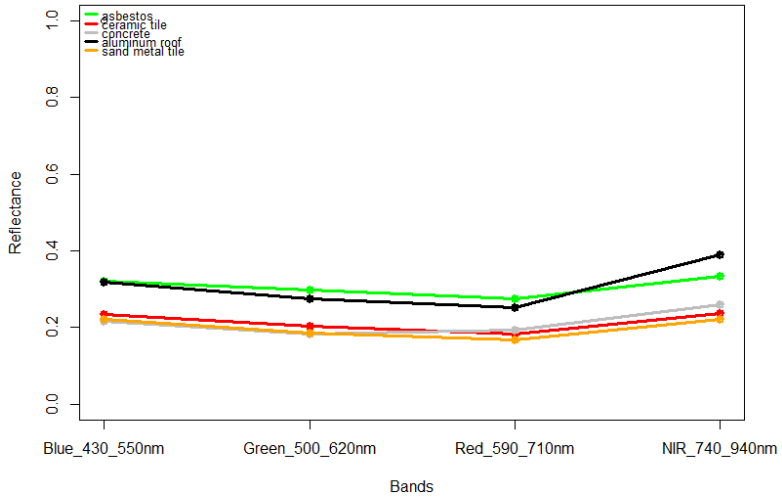

(a)

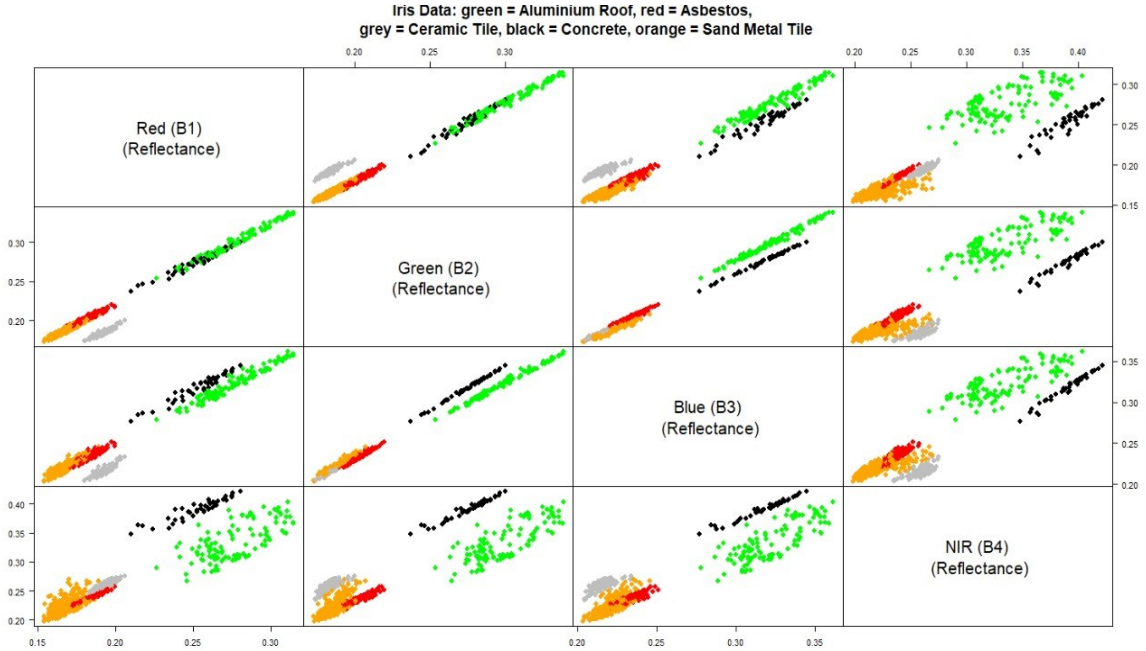

(b)

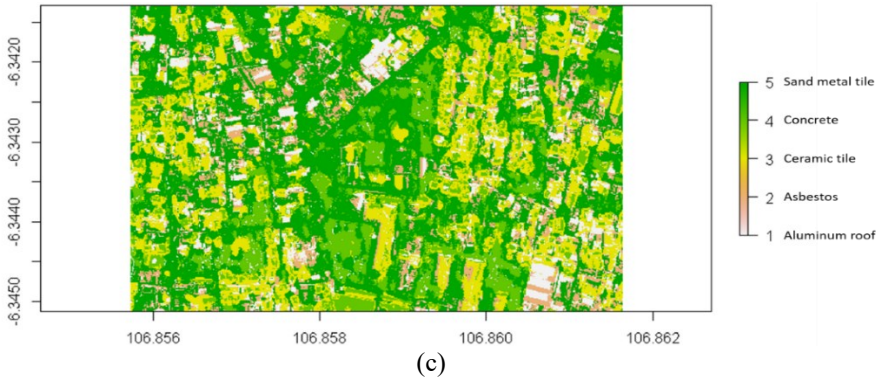

(c)

Figure 6. (a) Spectral reflectance profile from the Pleiades, (b) Scatter plot of spectral features, (c) Classification result

From Figure 8, we can see that the results are largely difficult to distinguish between sand metal tile, concrete, and vegetation. This is caused by several factors, among others; atmospheric correction that has not been applied, Pleiades imagery that only uses 4 (four), spectral bands, also spectral responses of sand metal tile and vegetation that have the same range. From the factors above, we tried to extract the Normalized Difference Vegetation Index (NDVI) value on the AOI used. We compare the results of NDVI (Figure 9 (a)) with our classification results, from there it is found that the vegetation areas that have not been separated from urban material are mostly detected as concrete or sand metal tiles. From these results, we do have a plan to do masking vegetation using the spectral index from NDVI for the next works. We also compared our findings with some spectral response references. For sand metal tile, we use a spectral response reference from sand because the material used on the roof is sand coated metal (Figure 9 (b)). As for concrete and vegetation we use the spectral response reference available on the ECOsystem Spaceborne Thermal Radiometer Experiment on Space Station (ECOSTRESS) spectral library website by NASA/JPL (Figures 9 (c), (d), (e)).

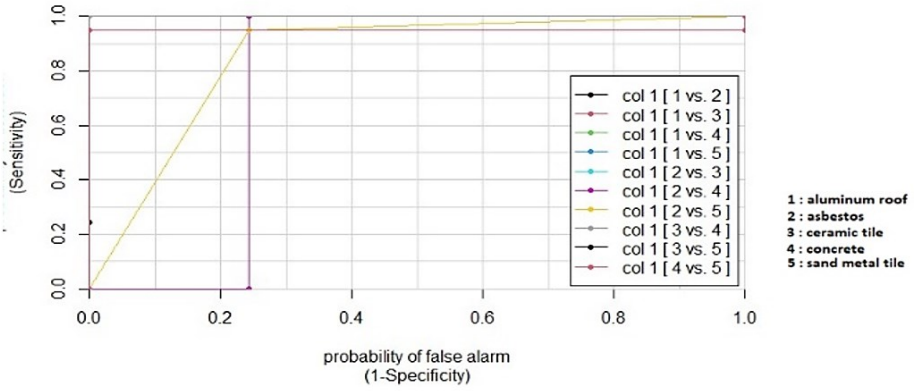

Figure 7. SVM ROC curve

Figure 8. Visual comparison of classification results with satellite image data
(red for model train data, and cyan for other objects that have been successfully detected)

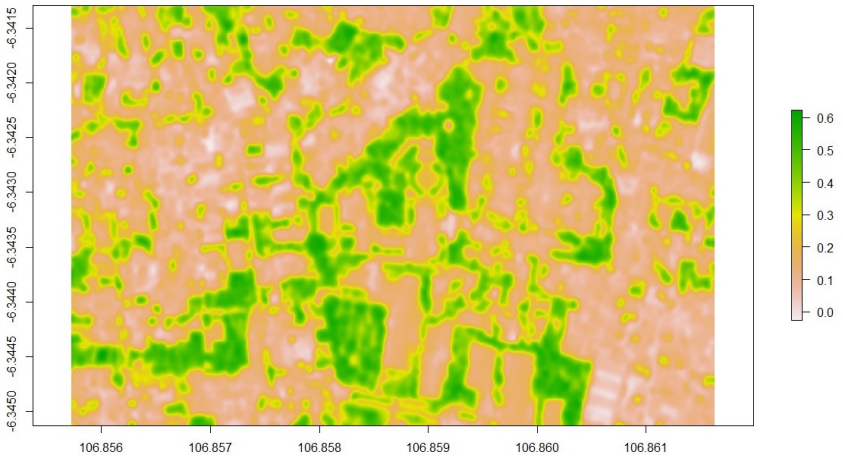

(a)

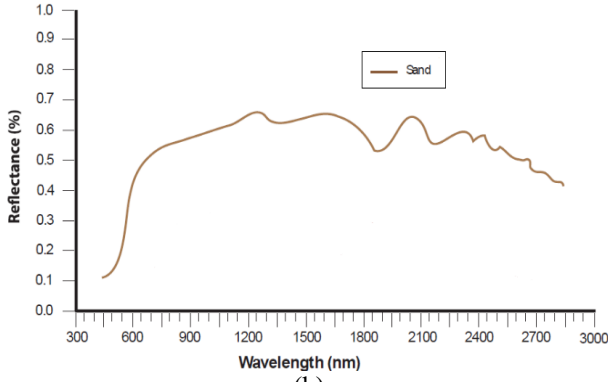

(b)

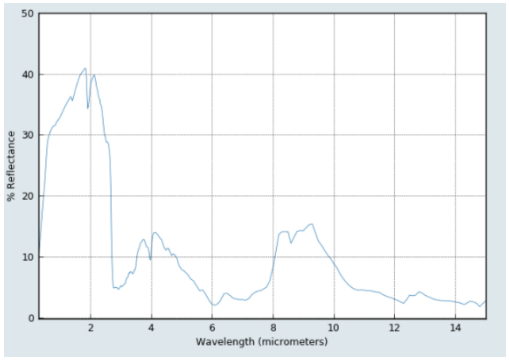

(c)

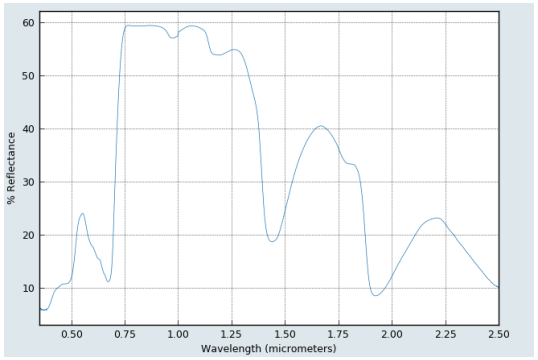

(d)

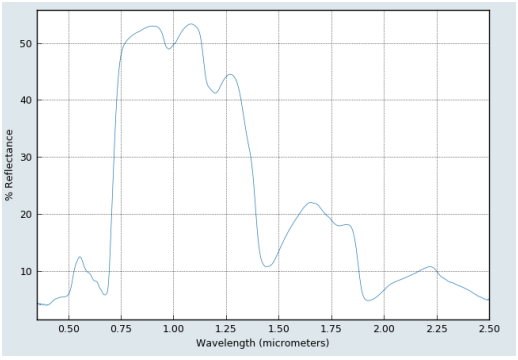

(e)

Figure 9. (a) NDVI result, (b) Sand spectral response, coating material for sand metal [44], (c) Concrete spectral response, (d) Spectral response of grass, (e) trees [45]

From the spectral response reference that we have, it appears that the responses produced by sand metal tile, concrete, and vegetation do have similarities, especially in the wavelength range of 750-1500 nm. This reinforces the reasons why the method we use is difficult to distinguish between sand metal tile, concrete, and vegetation in R, G, B, NIR bands. To overcome this shortcoming, we plan further research using the formulation of index values, from existing spectral values, which have greater differences between each other, data assimilation, and multilevel classification methods. For further verification, we have tried to use the method in different regions as a representative for much wider areas and variations, namely Purwokerto and Semarang. The data used for Purwokerto is cloud-free image data from the Pleiades satellite obtained on 30 January 2019, the detailed location is at Terminal Bulupitu. Meanwhile, the data used for Semarang is obtained on 3 May 2018, a detailed location is at State Polytechnic of Semarang. The results is shown in Table 6.

Figure 10 (a) and 10 (b) show SVM data and spectral reflectance profile from the Purwokerto region. Figures 11 (a) and 11 (b) show SVM data and spectral reflectance profile from the Semarang region. From the visual results and values generated by the SVM program, it appears that the method we proposed can classify aluminum roof, asbestos, ceramic tile, concrete, and sand metal tile materials. However, the spectral reflectance results also show a slightly different pattern from the results from the Jakarta area. In Table 7 it can be seen that there are significant results, especially in the asbestos material in Semarang. Based on Table 8, the overall accuracy and Kappa coefficient value on the method that we use are equal to 92.92% and 0.9069, this result is better if compared to previous studies that obtained an overall accuracy value of 83% and Kappa coefficient 0.76 to do roof detection using WorldView-2 satellite that has 8 (eight) multispectral bands [46]. Our result shows that field surveys are still needed in the Purwokerto and Semarang areas to ensure the type of roof materials available. The classification we did is also limited to just 5 (five) materials, so other unknown materials are identified as them instead. In future works, we plan to do the exhaustive field surveys, TOA bidirectional reflectance distribution function (BRDF), and vegetation masking, so that the identification can be upgraded into a better result with only urban roof material as a study area.

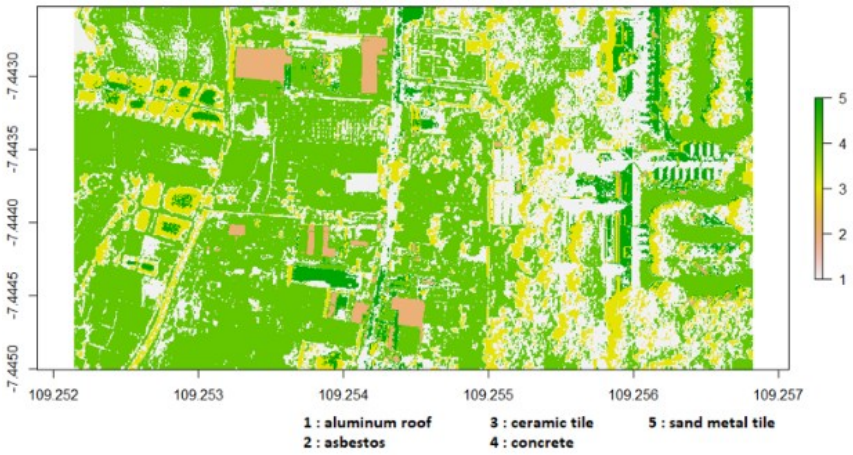

(a)

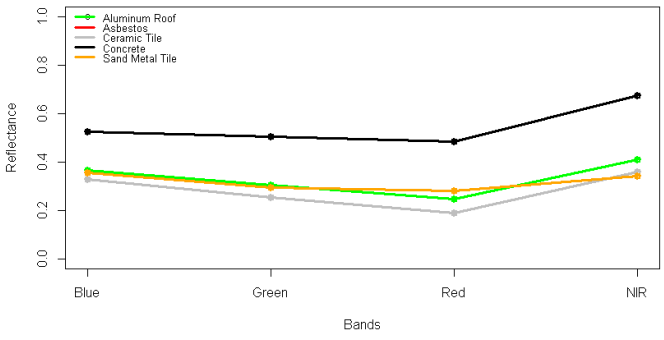

(b)

Figure 10. (a) SVM data of Purwokerto region; (b) Spectral reflectance profile of Purwokerto region

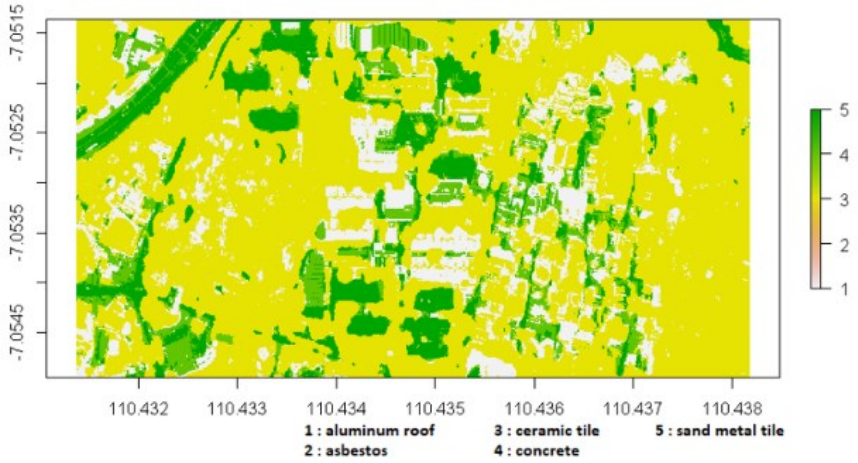

(a)

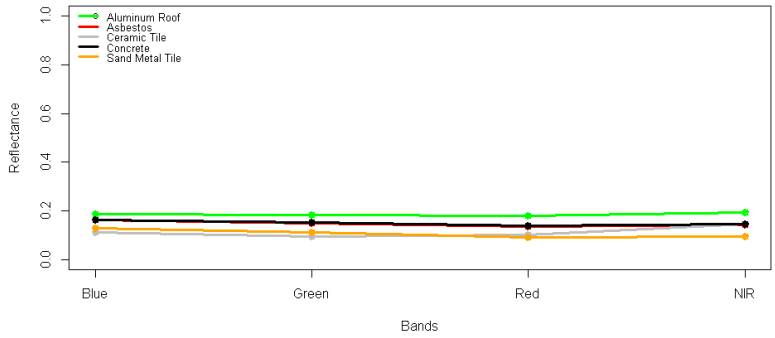

(b)

Figure 11. (a) SVM data of Semarang region, (b) Spectral reflectance profile of Semarang region

Table 6. Compared reflectance value at 3 regions

Materials	Band Reflectance Value			
	Blue	Green	Red	NIR
Aluminum Roof				
Jakarta	0.322	0.299	0.276	0.334
Purwokerto	0.367	0.306	0.245	0.410
Semarang	0.186	0.182	0.181	0.192
Asbestos				
Jakarta	0.234	0.204	0.183	0.237
Purwokerto	1.332	1.479	1.622	1.801
Semarang	0.162	0.149	0.135	0.141
Ceramic Tile				
Jakarta	0.215	0.184	0.192	0.260
Purwokerto	0.327	0.253	0.190	0.359
Semarang	0.111	0.094	0.102	0.146
Concrete				
Jakarta	0.317	0.275	0.253	0.390
Purwokerto	0.524	0.504	0.484	0.673
Semarang	0.162	0.153	0.140	0.146
Sand Metal Tile				
Jakarta	0.220	0.187	0.167	0.222
Purwokerto	0.356	0.295	0.281	0.342
Semarang	0.128	0.110	0.092	0.096

Table 7. Compared value of material types for some parameters at 3 regions

Parameters	Sensitivity	Specificity	Detection Rate	Balanced Accuracy
Aluminum Roof				
Jakarta	1	1	0.1553	1
Purwokerto	0.9779	0.9955	0.2277	0.9867
Semarang	0.9450	1	0.2077	0.9725
Asbestos				
Jakarta	0.7563	0.9756	0.1226	0.8660
Purwokerto	1	1	0.137	1
Semarang	0	1	0	0.5000
Ceramic Tile				
Jakarta	1	1	0.1948	1
Purwokerto	0.9800	0.9938	0.1678	0.9869
Semarang	1	1	0.2198	1
Concrete				
Jakarta	0.9525	0.9306	0.4101	0.9416
Purwokerto	1	1	0.2329	1
Semarang	0.9500	0.8296	0.2088	0.8898
Sand Metal Tile				
Jakarta	0.9525	0.9306	0.4101	0.9416
Purwokerto	1	1	0.226	1
Semarang	1	0.9859	0.2198	0.9930

Table 8. Compared value of overall accuracy and kappa coefficient at 3 regions

Parameters	Overall Accuracy (%)	Kappa Coefficient
Jakarta	94.01	0.9165
Purwokerto	99.14	0.9892
Semarang	85.60	0.8150
Mean	92.92	0.9069

4. CONCLUSION

The identification of roof materials has been carried out using the spectral response from the Pleiades data as the basis. The results show us that the classification successfully identified most of the materials in the study area. The overall accuracy and Kappa coefficient value on the method that we use are equal to 92.92% and 0.9069. However, our method has difficulty distinguishing sand metal tile, concrete, and vegetation. The cause is a similar spectral response range between sand metal tile, concrete, and vegetation. In future work, we will overcome this problem by formulating index values from existing spectral values which have greater differences between each other, vegetation masking, assimilation, multilevel, and multitemporal classification methods.

ACKNOWLEDGEMENTS

This research is supported by PRN Research Grant number 256/E1/PRN/2020 from the Ministry of Research and Technology – National Research and Innovation Agency.

AUTHOR CONTRIBUTIONS

AW conceived, planned the experiments, and took the lead in writing the manuscript. YFH carried out the experiments and the simulations. YDS and DM contributed to sample preparation, interpretation of the results, and wrote the manuscript with input from all authors. DI contributed to the recommendations for the use of data. R, DT, and ESA helped to review the paper and methodology. DI, R, DT, and ESA also helped supervise the project and encourage AW, YFH, YDS, DM to investigate and supervised the findings of this work. All authors provided critical feedback and helped shape the research, analysis, and manuscript.

REFERENCES

[1] R. Powell, D. Roberts, P. Dennison, and L. Hess, "Sub-pixel mapping of urban land cover using multiple endmember spectral mixture analysis: Manaus, Brazil," *Remote Sens. Environ.*, vol. 106, pp. 253–267, Jan. 2007.
[2] R. M. Cavalli, L. Fusilli, S. Pascucci, S. Pignatti, F. Santini, and Z. Industriale, "Hyperspectral Sensor Data Capability for Retrieving Complex Urban Land Cover in Comparison with Multispectral Data: Venice City Case Study (Italy)," *MDPI*, 2008, pp. 3299–3320.
[3] S. Bhaskaran, S. Paramananda, and M. Ramnarayan, "Per-pixel and object-oriented classification methods for mapping urban features using Ikonos satellite data," *Appl. Geogr.*, vol. 30, no. 4, pp. 650-665, 2010.
[4] W. Heldens, T. Esch, U. Heiden, and S. Dech, "A Potential of Hyperspectral Remote Sensing for Characterisation of Urban Structure in Munich," *Carsten Jürgens Remote Sens.*, 2008, pp. 94–103.
[5] S. R. P. Sitorus, C. Leonataris, and D. R. Panuju, "Analisis Pola Perubahan Penggunaan Lahan dan Perkembangan Wilayah di Kota Bekasi, Provinsi Jawa Barat," *Jurnal Ilmu Tanah dan Lingkungan*, vol. 14, no. April, pp. 21–28, 2012.
[6] A. Le Bris, N. Chehata, X. Briottet, and N. Paparoditis, "Spectral Band Selection for Urban Material Classification Using Spectral Band Selection for Urban Material Classification Using," *ISPRS Congr.*, vol. 3, no. 7, pp. 33–40, 2016.
[7] A. Jochem, H. Bernhard, M. Rutzinger, and N. Pfeifer, "Automatic Roof Plane Detection and Analysis in Airborne Lidar Point Clouds for Solar Potential Assessment," *Sensors (Basel),* vol. 9, no. 7, pp. 5241–5262, 2009.
[8] W. Heldens, U. Heiden, and T. Esch, "Can the Future EnMAP Mission Contribute to Urban," *Remote Sens*, vol. 3, no. 9, pp. 1817-1846, 2011. https://doi.org/10.3390/rs3091817.
[9] S. Kotthaus, T. E. L. Smith, M. J. Wooster, and C. S. B. Grimmond, "Derivation of an urban materials spectral library through emittance and reflectance spectroscopy," *ISPRS J. Photogramm. Remote Sens.*, vol. 94, pp. 194–212, 2014.
[10] C. Rosenzweig *et al.*, "Mitigating New York City's heat island with urban forestry, living roofs, and light surfaces," *86th AMS Annual Meeting*, 2006.
[11] Q. Weng, D. Quattrochi, and P. E. Gamba, *Urban Remote Sensing*. 2018.
[12] A. Lefebvre, C. Sannier, and T. Corpetti, "Monitoring Urban Areas with Sentinel-2A Data : Application to the Update of the Copernicus High Resolution Layer Imperviousness Degree," *MDPI*, 2016, pp. 1–21.
[13] P. Danoedoro and A. Zukhrufiyati, "Integrating Spectral Indices and Geostatistics Based on Landsat-8 Imagery For Surface Clay Content Mapping in Gunung Kidul Area, Yogyakarta, Indonesia," 2015.
[14] A. Lucieer, A. Stein, and P. Fisher, "Texture-based Segmentation of High-Resolution Remotely Sensed Imagery for Identification of Fuzzy Objects," 2005.

[15] R. N. Clark, "Spectroscopy of Rocks and Minerals, and Principles of Spectroscopy." John Wiley and Sons, Inc, New York, 1999, pp. 3–58.
[16] K. Segl, S. Roessner, and H. Kaufmann, "Determination of robust spectral features for identification of urban surface materials in hyperspectral remote sensing data," *Remote Sensing of Environment*, vol. 111, no. 4, pp. 537–552, 2007.
[17] F. D. Acqua *et al.*, "HySenS data exploitation for urban land cover analysis," *Annals of geophysics = Annali di geofisica*, vol. 49, no. 1, 2006.
[18] S. Roessner, K. Segl, U. Heiden and H. Kaufmann, "Automated differentiation of urban surfaces based on airborne hyperspectral imagery," in *IEEE Transactions on Geoscience and Remote Sensing*, vol. 39, no. 7, pp. 1525-1532, July 2001, doi: 10.1109/36.934082. S. Roessner, K. Segl, U. Heiden, and H. Kaufmann, "Automated Differentiation of Urban Surfaces Based on Airborne Hyperspectral Imagery," vol. 39, no. 7, pp. 1525–1532, 2001.
[19] A. Ibrahim, S. Tominaga, and T. Horiuchi, "A Spectral Invariant Representation of Spectral Reflectance," *Opt. Rev.*, vol. 18, no. 2, pp. 231–236, 2011.
[20] A. Hamedianfar, H. Z. M. Shafri, S. Mansor, and N. Ahmad, "Combining data mining algorithm and object-based image analysis for detailed urban mapping of hyperspectral images," *J. Appl. Remote Sens.*, vol. 8, no. 1, 2014.
[21] N. E. M. Nasarudin and H. Z. M. Shafri, "Development and Utilization of Urban Spectral Library for Remote Sensing of Urban Environment," *JUEE*, vol. 5, pp. 44–56, 2011.
[22] J.-D. L. A, B. A. Dewitt, S.-S. Lee, K.-J. Bhang, and J.-B. Sim, "Analysis of Concrete Reflectance Characteristics Using Spectrometer and Vnir Hyperspectral Camera," *ISPRS Congr,* vol. XXXIX, no. September, pp. 127–130, 2012.
[23] A. Braun, G. Warth, F. Bachofer and V. Hochschild, "Identification of roof materials in high-resolution multispectral images for urban planning and monitoring," *2019 Joint Urban Remote Sensing Event (JURSE)*, Vannes, France, 2019, pp. 1-4, doi: 10.1109/JURSE.2019.8809026.
[24] U. Heiden, W. Heldens, S. Roessner, K. Segl, T. Esch, and A. Mueller, "Landscape and Urban Planning Urban structure type characterization using hyperspectral remote sensing and height information," *Landsc. Urban Plan.*, vol. 105, no. 4, pp. 361–375, 2012.
[25] W. Dai, I. Wardlaw, Y. Cui, K. Mehdi, Y. Li, and J. Long, "Data Profiling Technology of Data Governance Regarding Big Data : Review and Rethinking," *Springer, Cham*, no. April 2016, pp. 439–450, 2017.
[26] W. Dai, K. Yoshigoe, and W. Parsley, "Improving data quality through deep learning and statistical models," *Springer, Cham*, no. In Information Technology-New Generations, pp. 515–522, 2018.
[27] W. Dai *et al.*, "Benchmarking Contemporary Deep Learning Hardware and Frameworks : A Survey of Qualitative Metrics," *IEEE*, no. IEEE First International Conference on Cognitive Machine Intelligence (CogMI), pp. 148–155, 2019.
[28] Z. Wang, A. C. Bovik, and L. Lu, "Why is image quality assessment so difficult?," *IEEE Int. Conf. Acoust. Speech, Signal Process.*, vol. 4, p. IV-3313, 2002.
[29] H. Hassanpour and S. A. Amiri, "Image Quality Enhancement Using Pixel-Wise Gamma Correction via SVM Classifier," *IJE Trans. B Appl.*, vol. 24, no. 4, pp. 301–311, 2011.
[30] Satellite Imaging Corporation, "Satellite Sensors," *Satellite Imaging Corporation*, 2017. [Online]. Available: https://www.satimagingcorp.com/satellite-sensors. [Accessed: 24-Feb-2020].
[31] Y. Ling, M. Ehlers, E. L. Usery, and M. Madden, "FFT-enhanced IHS transform method for fusing high-resolution satellite images," *ISPRS J. Photogramm. Remote Sens.*, vol. 61, no. 6, pp. 381-392, February, 2007.
[32] Pcigeomatics.com, "Cluster." [Online]. Available: https://www.rdocumentation.org/packages/raster/versions/3.3-13/topics/cluster. [Accessed: 26-Aug-2020].
[33] N. Hoang, "Image Processing-Based Recognition of Wall Defects Using Machine Learning Approaches and Steerable Filters," *Comput. Intell. Neurosci,* vol. 2018, pp. 1-18, 2018. Doi: 10.1155/2018/7913952.
[34] M. Wegmann, B. Leutner, and S. Dech, *Remote Sensing and GIS for Ecologists Using Open Source Software*. Pelagic Publishing, 2016.
[35] R. Fan, P. Chen, and C. Lin, "Working Set Selection Using Second Order Information for Training Support Vector Machines," vol. 6, pp. 1889–1918, 2005.
[36] Scikit-learn.org, "Support Vector Machines." [Online]. Available: https://scikit-learn.org/stable/modules/svm.html#classification. [Accessed: 26-Aug-2020].
[37] Rdocumentation.org, "Support Vector Machines." [Online]. Available: https://www.rdocumentation.org/packages/e1071/versions/1.7-3/topics/svm. [Accessed: 26-Aug-2020].
[38] D. Meyer, "Support Vector Machines," vol. 1, pp. 1–8, 2019.
[39] F. Markowetz, "Classification by Support Vector Machines," pp. 1–26, 2003.
[40] Pcigeomatics.com, "PANSHARP." [Online]. Available: https://www.pcigeomatics.com/geomatica-help/references/pciFunction_r/python/P_pansharp.html. [Accessed: 26-Aug-2020].
[41] Astrium, "SPOT 6 & SPOT 7 Imagery User Guide," no. July, 2013.
[42] L3HARRIS GEOSPATIAL, "Radiance vs. Reflectance." [Online]. Available: https://www.harrisgeospatial.com/Support/Self-Help-Tools/Help-Articles/Help-Articles-Detail/ArtMID/10220/ArticleID/19247/3377#:~:text=Radiance is the variable directly,from the object being observed.&text=Reflectance is the ratio of,It has no units. [Accessed: 26-Aug-2020].
[43] HSU GEOSPATIAL, "Spectral Reflectance." [Online]. Available: http://gsp.humboldt.edu/OLM/Courses/GSP_216_Online/lesson2-1/reflectance.html. [Accessed: 26-Aug-2020].
[44] S. K. Alavipanah *et al.*, "A Review : Remote Sensing Application in Evaluation of Soil Characteristics in Remote sensing application in evaluation of soil characteristics in desert areas," *Nat. Environ. Chang.*, vol. 2, no. November, pp. 1–24, 2016.

[45] NASA/JPL, "ECOSTRESS Spectral Library," *NASA/JPL*, 2018. [Online]. Available: https://speclib.jpl.nasa.gov/library. [Accessed: 09-Mar-2020].
[46] E. Taherzadeh and H. Z. M. Shafri, "Development of a Generic Model for the Detection of Roof Materials Based on an Object-Based Approach Using WorldView-2 Satellite Imagery," *Adv. Remote Sens.*, vol. 2013, no. December, pp. 312–321, 2013.

BIOGRAPHIES OF AUTHORS

Ayom Widipaminto, S.T, M.T. Senior Engineer at Remote Sensing Technology and Data Center, National Institute of Aeronautics and Space. He attended the Institut Teknologi Bandung and graduated with a Bachelor's degree in Electrical Engineering. He got the opportunity to continue his Master's study at the University of Indonesia with Electrical Engineering as the majority. Currently, he is enrolling a Doctoral degree in the Department of Physics, Faculty of Mathematics and Sciences, University of Indonesia.

Yohanes Fridolin Hestrio, S.Si. Assistant Researcher at Remote Sensing Technology and Data Center, National Institute of Aeronautics and Space. He enrolled in a bachelor's degree in Physics Instrumentation from the University of Indonesia. Currently focusing on material urban identification using machine learning.

Yuvita Dian Safitri, S.S.T. Assistant Engineer at Remote Sensing Technology and Data Center, National Institute of Aeronautics and Space. She enrolled in a bachelor's degree in Telecommunication Engineering from the State Polytechnic of Semarang. Currently focusing on material urban identification using machine learning.

Donna Monica, S.Mat. Assistant Researcher at Remote Sensing Technology and Data Center, National Institute of Aeronautics and Space. She enrolled in a bachelor's degree in Mathematics from the University of Soedirman. Currently focusing on material urban identification using machine learning.

Ir. Dedi Irawadi. Head of Remote Sensing Technology and Data Center, National Institute of Aeronautics and Space. He graduated with a Bachelor's degree in Electrical Engineering from Texas A&M University. Currently focusing on material urban identification using machine learning and RF Engineering.

Dr. Rokhmatuloh, S.Si, M.Eng. Dean Faculty of Mathematics and Sciences, University of Indonesia. He attended the Department of Geography, University of Indonesia, and graduated in 1996 with a Bachelor's degree in Geography. He got the opportunity to continue his study at Chiba University supported by Monbukagakusho, Japan. At Chiba University, he enrolled at the Center for Environmental Remote Sensing (CEReS). Currently, he holds a Ph.D. degree in remote sensing from Chiba University, Japan. His lecture subjects including the application of remote sensing and GIS for disaster mitigation, regional development, environmental management, and digital image interpretation for undergraduate and master levels.

Dr. techn. Djoko Triyono, S.Si., M.Si. Deputy Dean for Education, Research and Student Affairs, University of Indonesia. S1 and S2 titles he received in the Department of Physics, University of Indonesia. Whereas for S3 degree he received in the field of materials physics, University of Vienna, Austria dissertation entitled "Development of New Materials Nano-Composite Soft-FE-based Magnets (Al-Ga) and Application for Intelligent Materials", 2005.

Prof. Dr. Ir. Rr. Erna Sri Adiningsih, M.Si. Main Secretary of National Institute of Aeronautics and Space. She attended Meteorology major at Bogor Agricultural Institute for a bachelor's degree. The master title is received from the Natural and Environmental Resource Management study at Bogor Agricultural Institute, and she holds a Doctoral degree in Climatology from Bogor Agricultural Institute. Currently focusing on material urban identification using machine learning.